Proceedings of the XV-th National School "Hundred Years of Superconductivity", Kazimierz Dolny, October 9–13, 2011

Superconducting Properties of VN–SiO_2 Sol–Gel Derived Thin Films

B. Kościelska[a,*], O.I. Yuzephovich[b,c], S.V. Bengus[b,c], A. Winiarski[d], W. Sadowski[a] and M. Łapiński[a]

[a]WFaculty of Applied Physics and Mathematics, Gdansk University of Technology
Narutowicza 11/12, 80-233 Gdańsk, Poland

[b]B. Verkin Institute for Low Temperature Physics and Engineering, NAS of Ukraine, Kharkov 61103, Ukraine

[c]International Laboratory of High Magnetic Fields and Low Temperatures, Gajowicka 95, 53-421 Wrocław, Poland

[d]A. Chełkowski Institute of Physics, University of Silesia, Uniwersytecka 4, 40-007 Katowice, Poland

In this work studies of structure and superconducting properties of VN–SiO_2 films are reported. The films were obtained through thermal nitridation (ammonolysis) of sol–gel derived V_2O_3–SiO_2 coatings (in a proper V_2O_3/SiO_2 ratio) at 1200°C. This process leads to the formation of disordered structure with VN metallic grains dispersed in the insulating SiO_2 matrix. The structural transformations occurring in the films as a result of ammonolysis were studied using X-ray photoelectron spectroscopy (XPS). The critical superconducting parameters are obtained. The magnetoresistance at high magnetic fields has been investigated.

PACS: 81.20.Fw, 74.78.–w

1. Introduction

Vanadium nitride is suitable for many uses due to its extreme hardness, wear resistance, excellent oxidative stability, corrosion resistance and high-temperature stability. From technological point of view, because of its good selectivity and stability [1, 2], VN is an important industrial catalyst. Moreover VN is a superconductor with a transition temperature ≈ 9 K [3, 4] and may be used in several superconducting microelectronics applications.

Thin films consisting of VN are usually prepared by magnetron sputtering method, physical or chemical vapour deposition and by heating vanadium metal in a nitrogen atmosphere at high temperature. Another very promising method of the nitride and oxynitride films preparation is a thermal nitridation (with ammonia) of sol–gel derived metal–oxide films. The coatings obtained by sol–gel method are especially suitable for the ammonolysis because of their porosity. The microporous structure allows both a significant incorporation of nitrogen and its distribution through the film. Homogeneous distribution of nitrogen is very important, because the presence of zone with nitrogen deficiency or excess can change properties of the layer. An excellent precursor to obtain VN using above method seems to be V_2O_3. The ammonolysis of sol–gel derived V_2O_3–SiO_2 leads to the formation of VN grains dispersed in SiO_2 matrix. Such granular systems are very interesting from the point of view of the mechanisms of electrical conductivity, relationships between normal and superconducting state and the interplay between local and global superconductivity.

This work is devoted to the structure and superconducting properties of xVN–(100–x)SiO_2 (where $x = 90$, 80, 70, 60 and 50 mol%) films, prepared by thermal nitridation of sol–gel derived V_2O_3–SiO_2 coatings.

2. Experimental

The films with a composition xVN–(100–x)SiO_2 (where $x = 90$, 80, 70, 60 and 50 mol%) were obtained by thermal nitridation of V_2O_3–SiO_2 sol–gel derived films (in a proper V_2O_3/SiO_2 ratio) with ammonia. The starting solution was prepared by mixing tetraethoxysilane (TEOS, 98%) from Fluka and vanadium (V) oxytripropoxide (98%) from Aldrich with ethanol and acetyloacetone as the complexing agent. The green colour of the as prepared solution was caused by V^{3+} species. The films were deposited on the silica glass substrate by a spin coating technique at a rate of 100 rps, then aged and heated at 250°C for 1 h. Repeating the above procedure three times gave (after ammonolysis) approximately 450 nm thick films. The thickness of the samples was determined using profilometer. To obtain VN–SiO_2 coatings, the resulting V_2O_3–SiO_2 layers were

* corresponding author; e-mail: basia@mif.pg.gda.pl

subsequently nitrided by ammonia treatment at the temperature 1200°C. The nitridation was carried out in a silica glass tube under NH_3 gas flow (4 l/h) at a heating rate of 1°C/minute from the room temperature to 1200°C and then held isothermally at this temperature for 1 h. After that the samples were cooled under NH_3 gas flux.

AFM images were taken with Bruker AFM-NanoScope.

XPS spectra were recorded with a multipurpose electron spectrometer PHI 5700/660 from Physical Electronics using monochromatized AlKα radiation. The anode was operated at 15 kV and 225 W. Low and high resolution spectra were measured. The binding energies were corrected using the background C1s line (285.0 eV) as a reference [5]. MultiPak program was used to fit high-resolution spectra. Mixed Gaussian and Lorentzian functions and Shirley background were applied.

Magnetotransport measurements were performed in the temperature range 1.4–300 K in a standard Oxford Instruments helium cryostat equipped with the 14 T superconducting solenoid. The temperature was stabilized using Lake Shore 340 temperature controller with the accuracy 0.001 K at $T < 10$ K and 0.01 K at $T > 10$ K. The resistance measurements were carried out using standard four-probe technique. Both DC and AC (50 nA, 13 Hz) measurements were made. The transport current $\boldsymbol{I}$ was parallel to the plane of the sample with the condition $\boldsymbol{I} \perp \boldsymbol{H}$. The transition temperature T_c and the upper critical magnetic fields H_{c2} were defined from the resistive transitions by the criterion $R = 0.5R_n$.

3. Results and discussion

The AFM image of $x = 70$ sample is shown in Fig. 1. This sample exhibits regularly shaped nanocrystals of the same size about 30 nm. The structure of the other samples is less regular, with the different size of the grains. As it was shown in XRD results [6] the main crystalline phase formed in the samples is VN. No peaks arising from crystalline SiO_2 or silicon nitrates and oxynitrides were observed. It may suggest, that the grains seen in Fig. 1 correspond to VN crystalline phase.

The exemplary XPS spectra of $x = 70$ sample after ammonolysis at 1200°C are presented in Fig. 2a, b and c. In V2p region (Fig. 2a), apart of the peaks in positions 513.79 eV and 521.39 eV attributed to VN (respectively to V2$p_{3/2}$ and V2$p_{1/2}$), also the peaks close to those reported for vanadium oxides (516.45 eV and 524.05 eV) are present [7–11]. This suggests that the transition from V_2O_3 to VN is not finished yet. Peaks in energy positions 530.29 eV and 532.28 eV correspond to O1s region. If to compare $V2p$ region of $x = 70$ with the same regions of $x = 50$ and $x = 90$ films (Fig. 3a), it may be noticed that in $x = 70$ sample VN phase is most significant. It can be concluded that SiO_2 addition to the samples may influence on formation of the VN phase. It seems to be possible, that microporous system, created before nitridation process, is more extended in the samples containing higher quantity of silica. The microporous structure allows both a significant incorporation of nitrogen and its distribution through the film. This finally leads to VN phase increase in $x = 70$ sample. From the other side, the largest number of vanadium oxide forms is present in $x = 50$ sample. In this sample VO_2, V_2O_3, and V_2O_5 are observed [7, 8]. It may be also possible, that too extended SiO_2 micropourous system can block nitrogen transfer trough the film. Closing during ammonolysis process porous trap ammonia molecules, what finally makes V_2O_3 to VN transformation not possible. Despite the fact that vanadium oxide phases are visible in XPS results, their amount is not large. Only VN crystalline phase was seen in XRD results of the films [6]. Si 2p region of the spectrum is shown in Fig. 2b. The best fit is reached for two different energy peaks corresponding to Si_xN_y [12] and SiO_2 [7]. This indicates that at 1200°C some Si–N bonds are formed. In Si 2p region of energy H_2O presence was also noticed. Comparison with other samples indicates, that SiO_2 phase is most visible in $x = 50$ sample (Fig. 3b). In N1s region only two peaks are present (Fig. 2c). The peak at lower energy position may be associated to VN and SiN_x whereas the higher energy peak may be identified as NH_3 [11]. NH_3 peak is most significant in $x = 50$ sample (Fig. 3c). It can be caused by the sample preparation way.

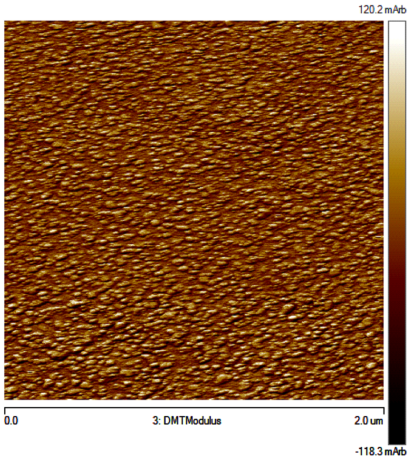

Fig. 1. The AFM image of $x = 70$ sample. The image was taken in DMT modulus.

Preliminary results of superconducting properties studies were obtained on two samples with $x = 60$ and $x = 80$. The critical temperatures T_c are about 7 K for both samples and are a little bit lower than reported in the literature. It may be caused by the sample preparation method. Even small deviation from stoichiometry or the presence of V–O bonds in the system can decrease critical temperature [13].

Magnetoresistance curves at different temperatures in the perpendicular magnetic field $H_\perp$ for $x = 80$ sample and $H_\parallel$ for $x = 60$ sample in the parallel magnetic

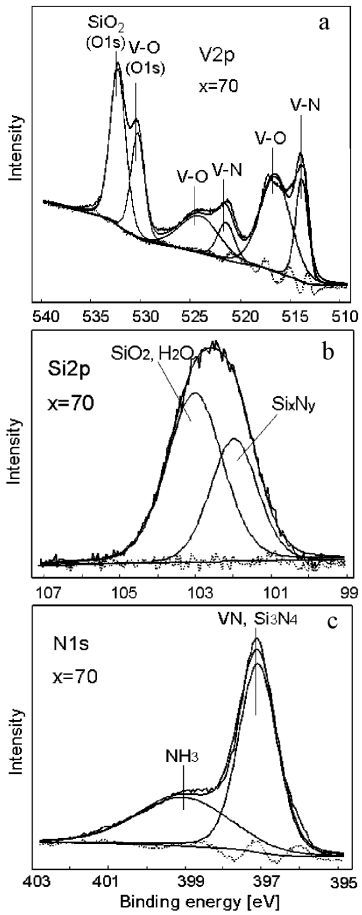

Fig. 2. (a) V2p and O1s spectra of $x = 70$ sample; (b) Si2p spectrum of $x = 70$ sample; (c) N1s spectrum of $x = 70$ sample.

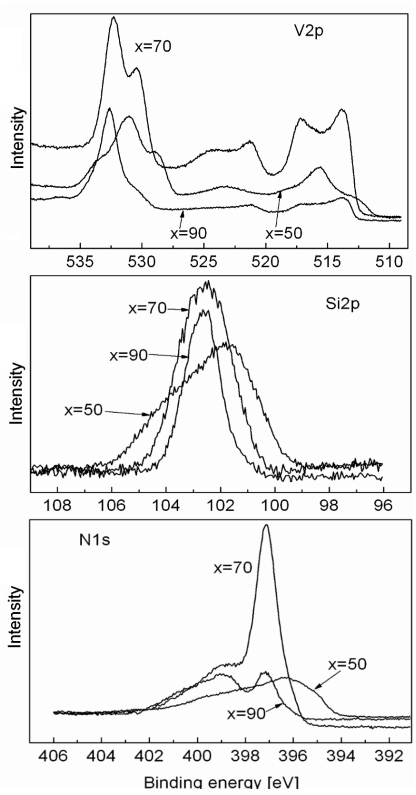

Fig. 3. (a) Comparison of V2p and O1s regions of $x = 50$, 70 and 90 films; (b) Comparison of Si2p region of $x = 50$, 70 and 90 films; (c) Comparison of V2p region of $x = 50$, 70 and 90 films.

field are shown in Fig. 4 and Fig. 5 respectively. For $x = 80$ and $x = 60$ the superconductor–insulator transition is not observed in contrast to granular NbN-SiO_2 films [14]. Also no broadening of the superconducting resistive transitions is found even in high magnetic fields.

Figure 6 shows the upper critical field for $x = 60$ and $x = 80$ samples. Upper critical fields were determined from the $R(H)$ curves. The $H_{c\perp}(0)$ at $T = 0$ K is about 14 T for a bulk material and determined from the linear (3D) segment extrapolation of the $H_{c\perp}(T)$ curve for $x = 80$ sample. The parallel critical field has no such linearity. The parallel coherence length $\xi_{\|}(0)$ at $T = 0$ is equal to 6 nm. It was obtained from the $H_{c\perp}(T)$ using Ginzburg–Landau equation. Details of the behavior of magnetoresistance and critical magnetic fields will be discussed in the next article.

4. Conclusions

Thermal nitridation of V_2O_3–SiO_2 sol–gel derived films (in a proper V_2O_3/SiO_2 ratio) with ammonia leads to the formation of VN grains dispersed in SiO_2 matrix.

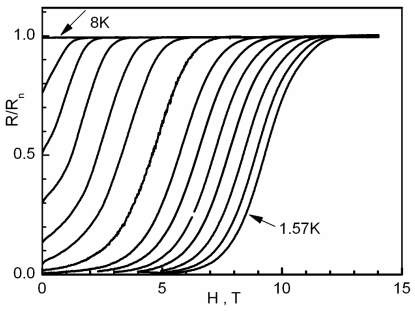

Fig. 4. Magnetoresistance of the sample $x = 80$ in the perpendicular magnetic field at different temperatures: 1.57 K, 2.0 K, 2.51 K, 2.94 K, 3.34 K, 3.81 K, 4.22 K, 4.9 K, 5.5 K, 6.0 K, 6.5 K, 7 K, 7.3 K, 8 K.

Critical temperatures of prepared with this method superconducting films are a little bit lower than reported in the literature. It may be caused by the sample preparation method. Even small deviation from stoichiometry or the presence of V–O bonds in the system can decrease critical temperatures. Though there is a little difference between the critical temperatures of superconducting transition of our films and the films prepared by other methods, our method allows making films of any shape and controlling the size of granules. Moreover,

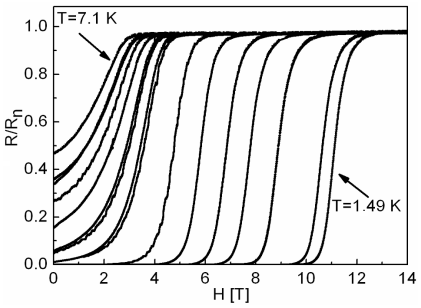

Fig. 5. Magnetoresistance of $x = 60$ sample in the parallel magnetic field at different temperatures: 1.49 K, 2.12 K, 3.53 K, 4.24 K, 4.7 K, 3.56 K, 5.3 K, 5.8 K, 6.3 K, 6.4 K, 6.7 K, 6.8 K, 6.9 K, 7 K and 7.1 K.

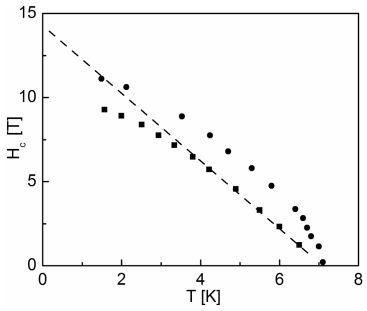

Fig. 6. Upper critical fields of $x = 60$ (circles) and $x = 80$ (squares) samples versus temperature.

these films have rather high critical magnetic fields for low-temperature superconductors. Therefore, films prepared with this method may be used in superconducting microelectronics applications.

Acknowledgments

This work was supported in part by the targeted comprehensive program for basic research of the National Academy of Sciences of Ukraine entitled "Fundamental problems in nanostructured systems, nanomaterials, and nanotechnologies" grant No. 26/11-N.

Authors would like to thank Bruker Corporation for AFM examinations.

References

[1] S.T. Oyama, *Catal. Today* **15**, 1 (1992).

[2] H. Kwon, S. Choi, L.T. Thompson, *J. Catal.* **184**, 236 (1999).

[3] B.R. Zhao, L. Chen, H.L. Luo, M.D. Jack, D.P. Mullin, *Phys. Rev. B* **29**, 6198 (1984).

[4] K.E. Gray, R.T. Kampwirth, D.W. Capone, II, R. Vaglio, J. Zasadzinski, *Phys. Rev. B* **38**, 2333 (1988).

[5] B.V. Crist, *Handbook of Monochromatic XPS Spectra*, XPS International Inc. Japan., 1999.

[6] B. Kościelska, A. Winiarski, W. Jurga, *J. Non-Cryst. Solids* **356**, 1998 (2010).

[7] Handbook of X-ray Photoelectron Spectroscopy, Eds. C.D. Wanger, W.M. Riggs, L.E. Davis, J.F. Moulder, G.E. Muilenberg, Perkin-Elmer Corp., Physical Electronics Division, Eden Prairie (MI) 1979.

[8] S. Surnev, M.G. Ramsey, F.P. Netzer, *Prog. Surf. Sci.* **73**, 117 (2003).

[9] J. Mendialdua, R. Casanova, Y. Barbaux, *J. Electron Spectrosc. Relat. Phenom.* **71,** 249 (1995).

[10] R. Sanjinés, C. Wiemer, P. Hones, F. Lévy, *J. Appl. Phys.* **83**, 1396 (1998).

[11] Z. Zhao, Y. Liu, H. Cao, J. Ye, S. Gao, M. Tu, *J. Alloys Compd.* **464**, 75 (2008).

[12] D.E. Starr, F.M.T. Mendes, J. Middeke, R.P. Blum, H. Niehus, D. Lahav, S. Guimond, A. Uhl, T. Kluener, M. Schmal, H. Kuhlenbeck, S. Shaikhutdinov, H.-J. Freund, *Surf. Sci.* **599**, 14 (2005).

[13] B.W. Roberts, *J. Phys. Chem. Ref. Data* **5**, 581 (1976).

[14] O.I. Yuzephovich, S.V. Bengus, B. Kościelska, A. Witkowska, *Low Temp. Phys.* **36**, 1058 (2010).